Towards Copper(I) Clusters for Photo-Induced Oxidation of Biological Thiols in Living Cells**

Gourdon-Grünewaldt, Lisa ; Blacque, Olivier ; Gasser, Gilles ; Cariou, Kevin

DOI: https://doi.org/10.1002/cbic.202300496

ChemBioChem

Research Article
doi.org/10.1002/cbic.202300496

Chemistry Europe
European Chemical Societies Publishing

www.chembiochem.org

Special Collection

Towards Copper(I) Clusters for Photo-Induced Oxidation of Biological Thiols in Living Cells**

Lisa Gourdon-Grünewaldt,[a] Olivier Blacque,[b] Gilles Gasser,*[a] and Kevin Cariou*[a]

The cell redox balance can be disrupted by the oxidation of biological peptides, eventually leading to cell death, which provides opportunities to develop cytotoxic drugs. With the aim of developing compounds capable of specifically inducing fatal redox reactions upon light irradiation, we have developed a library of copper compounds. This metal is abundant and considered essential for human health, making it particularly attractive for the development of new anticancer drugs. Copper(I) clusters with thiol ligands (including 5 novel ones) have been synthesized and characterized. Structures were elucidated by X-ray diffraction and showed that the compounds are oligomeric clusters. The clusters display high photooxidation capacity towards cysteine – an essential amino acid – upon light irradiation in the visible range (450 nm), while remaining completely inactive in the dark. This photoredox activity against a biological thiol is very encouraging for the development of anticancer photoredox drugs.The *in vitro* assay on murine colorectal cancer cells (CT26) did not show any toxicity – whether in the dark or when exposed to 450 nm light, likely because of the poor solubility of the complexes in biological medium.

Introduction

Medicinal inorganic chemistry is a dynamic and versatile research field that has gained significant attention lately.[1] One notable compound in this category is cisplatin, an anticancer drug discovered over 50 years ago.[2] Despite their effectiveness, these drugs often come with significant side effects. One way to address this issue is to use inactive prodrugs that can be specifically activated when needed by an external stimulus, such as light. This allows precise control over the drug's activation in terms of both location and time. Photodynamic therapy (PDT) is a clinically approved technique based on a photosensitizer (PS), light and endogenous O_2.[5] However, this dependence on O_2 concentration can be problematic, especially in the case of tumors that are often hypoxic at their core. In 2019, a phototoxic iridium(III) photooxidative catalyst was developed, which demonstrated activity against both normoxic and hypoxic cancer cells.[6] Upon light irradiation, this compound catalytically oxidized NADH, an important coenzyme, generating $NAD^{\bullet}$ radicals and reducing cytochrome c. The resulting depletion of NADH and redox imbalance led to the apoptosis of cancer cells upon 450 nm irradiation. While this approach was groundbreaking, iridium is a rare and expensive metal. From this point of view, working with a first-row transition metal would be more sustainable and less costly.[7] The numerous advantages of 1st-row transition metals (price, abundance) are however counterbalanced by the difficulty of modulating their photochemical properties[8] in order to design PS suitable for PDT. Copper is an abundant metal whose trade has been documented for almost 4000 years,[9] and which has already led to promising results in PDT. We thus decided to study copper-based structures for light-induced oxidation, in particular with the aim to trigger potentially cytotoxic oxidative events with various free radicals, as an alternative to oxygen dependency.

To achieve efficient intracellular photoredox catalysis for therapeutic and anticancer purposes, a PS with a long-lasting excited state is required. This PS should be capable of reacting with vital endogenous species in the cell upon light irradiation and producing toxic species like radicals, while also being able to return to its ground state and be regenerated. Our targets in this study are cysteine, an essential amino acid, and glutathione (GSH), an essential peptide. Both can be oxidized into a dimer by forming a disulfide bond. By oxidizing one or the other, we can disrupt the redox imbalance in the cell, eventually leading to apoptosis.[10]

The cytotoxicity of the reaction between Cu(II) and GSH has long been known.[11,12] Moreover, the oxidation of Cu(I) to Cu(II) can produce ROS, toxic to cells. Several groups have shown that a Cu(I) complex can be photoexcited to generate a long-lived triplet state of the Cu(I) species, with partial separation of the

[a] L. Gourdon-Grünewaldt, Prof. Dr. G. Gasser, Dr. K. Cariou
Institute of Chemistry for Life and Health Sciences
Laboratory for Inorganic Chemical Biology
Chimie ParisTech, PSL University, CNRS
11 rue Pierre et Marie Curie, 75005 Paris (France)
E-mail: kevin.cariou@chimieparistech.psl.eu
gilles.gasser@chimeparistech.psl.eu

[b] Dr. O. Blacque
Department of Chemistry
University of Zurich
Winterthurerstrasse 190, 8057 Zurich (Switzerland)

[**] A previous version of this manuscript has been deposited on a preprint server (https://doi.org/10.26434/chemrxiv-2023-qxlgg)

Supporting information for this article is available on the WWW under https://doi.org/10.1002/cbic.202300496

Special Collection This article is part of the SCF-ChemBio: Chemical Biology Tour de France Special Collection. Please see our homepage for more articles in the collection.

charge by transfer between the ligand and the metal. Thanks to this charge transfer, an electron can be given to the oxygen (Single Electron Transfer mechanism) to generate the superoxide radical anion ($O_2^{\bullet-}$) and an electron-deficient Cu(II) complex. However, this process has mainly been used for synthetic methodology development in photoredox catalysis.[13] In a biological context, the superoxide radical anion could oxidize GSH to GSSG (See Scheme 1). This would constitute a first GSH oxidation route. Subsequently, the Cu(II) species may itself be able to interact with GSH in a SET process. This second GSH oxidation pathway would thus close the catalytic cycle by regenerating the Cu(I) species in its ground state.

Copper(II) species are well-known for their ability to oxidize biological molecules such as the sulfur-containing peptide GSH or cysteine.[14–17] Therefore, it is crucial to design a PS that is not in the +2 oxidation state in the ground state to avoid dark toxicity. That is why we chose to synthesize copper(I) compounds that would display oxidizing capacity only when irradiated with light. The proposed catalytic cycle for this photocatalysis reaction is shown in Scheme 1. Of note, in a cellular setup in the absence of oxygen, cytochrome *c* could play the role of the Cu(I) to Cu(II) oxidant, as previously reported for Ir.[6]

In this article, we present the synthesis and characterization of a family of copper(I) pyrimidine thiol oligomeric clusters. Their ability to oxidize cysteine and GSH upon 450 nm irradiation and their photocytotoxicity on murine colorectal cancer cells (CT26) was also studied.

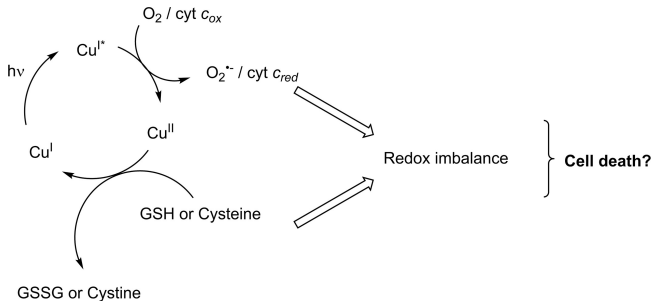

Scheme 1. Catalytic cycle proposed for the photooxidation capacity of Copper(I) clusters to induce cell death.

Results and Discussion

Synthesis and characterization

The ligands chosen for coordinating copper(I) are hybrid ligands with different coordination sites, with soft and hard donors. *N,S*-donor ligands such as pyridine-2-thiol or pyrimidine-2-thiol have already been extensively used for coordinating copper(I) complexes.[18,19] The synthesis of copper(I) clusters with one ligand of this type has previously been reported by Zhang *et al* and showed photooxidative properties for the conversion of phenylboronic acids into phenols.[20] In the present study, novel derivatives with thiol ligands appended with a variety of aromatic moieties (phenol for **L2**, anisole for **L3**, chlorobenzene for **L4**, benzodioxole for **L5**, methanesulfonylbenzene for **L6**) were synthesized in order to probe their effect on the redox activity and solubility. Those ligands were synthesized in two steps (Scheme 2). First, the double condensation of the phenylacetic acid (eventually substituted) with the Vilsmeier reagent (formed *in situ*) gave an vinylogous amidinium (vinamidium), which was isolated as its hexafluorophosphate salt (**V1**–**V6**). The reaction was carried out in DMF at 90 °C using 3 equivalents of $POCl_3$. In a second step, these vinamidinium salts were refluxed with 1.5 equivalent of thiourea and 2 equivalents of MeONa in MeOH. After cooling to room temperature (r.t.), the addition of acetic acid gave the ligands as yellow powders in good yields (**L1**–**L6**).

Then, we carried out the solvothermal reactions of copper bromide with the previously reported ligands in MeCN at 120 °C under an inert gas atmosphere, with a drop of Et_3N to yield the desired complexes. Two different approaches have been explored for the synthesis of the copper clusters **1Cu**–**6Cu**. To obtain crystals suitable for X-ray characterization, the solvothermal reaction was performed with a programmable oven (120 °C for 48 h followed by a decreased of temperature of 5 °C/h to r.t.), and, for easier scale-up, the same reaction has been

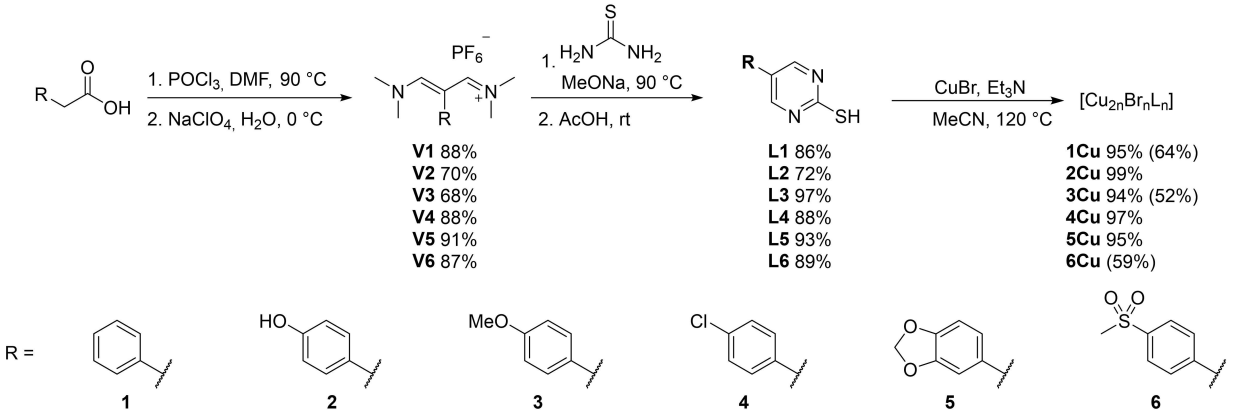

Scheme 2. Synthesis of vinamidinium salts **V1**–**V6**, of ligands **L1**–**L6** and of copper clusters **1Cu**–**6Cu**. Yields are indicated for the synthesis of amorphous powders (in brackets for the synthesis of crystals).

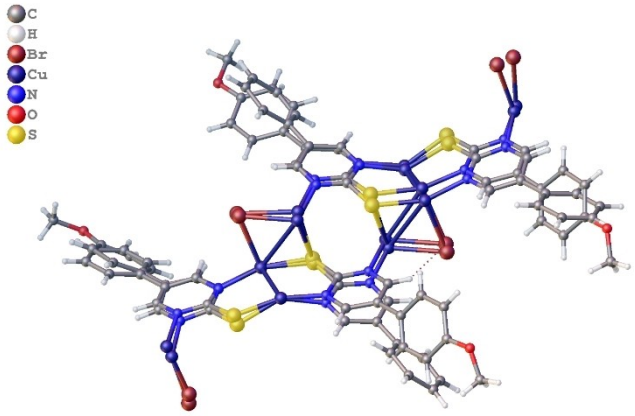

Figure 1. Overlay drawing of the molecular structures of **1Cu** and **3Cu**.

performed in a pressure tube, but without the slow decrease of temperature, which yielded red amorphous powders.

All compounds have been characterized by UV-visible absorption in acetonitrile, showing intense bands around 280 nm and 350 nm, with an absorption tail going up to 450 nm. The elemental analysis guided us to confirm the similar ligands/copper/bromide ratio between crystalline and amorphous forms. The IR spectra were recorded in solid form and in DMSO, showing similar peaks (see Supplementary Information). The clusters are stable towards oxygen and moisture over a three-month range. However, all clusters are very poorly soluble in most organic solvents and water.

The +1 oxidation state of the cluster was inferred from the NMR spectra, which do not seem to show copper(II) paramagnetic species (Figures S12–S17). Moreover, cyclic voltammetry in MeCN with NBu_4PF_6 as a supporting electrolyte allowed us to confirm the +1 oxidation state of one representative compound **4Cu** (Figure S42). However, the oxidation signal observed was very weak, which might be due to the very slow diffusion of such oligomeric species.

X-Ray crystallography

The solvothermal reaction under an inert gas atmosphere in a programmable oven (120 °C for 48 h followed by a decrease of temperature of 5 °C/h to r.t.) yielded the desired compounds as red crystals for **1Cu**, **3Cu** and **6Cu**. The X-ray diffraction study carried out on the single crystals of **1Cu** revealed the same crystal structure previously reported by Zhang et al.[20] In that structure, the copper(I) 5-phenylpyrimidine-2-thiolate (5-phpymt) complex forms a two dimensional polymer $[Cu_4(\mu5\text{-}5\text{-}phpymtH)_2(\mu\text{-}Br)_2]n$ in which one dimensional $[Cu_8(\mu\text{-}Br)_2(\mu5\text{-}5\text{-}phpymt)_4]n$ chains are connected by μ-Br– ions. A more detailed description of the original crystal structure is proposed in their manuscript.[14] Interestingly, the analysis of the crystals of **3Cu** and **6Cu** revealed structures very similar to **1Cu** built from the two dimensional polymers $[Cu_4(\mu5\text{-}5\text{-}(4\text{-}methoxyphpymt)_2(\mu\text{-}Br)_2]n$ and $[Cu_4(\mu5\text{-}5\text{-}(4\text{-}methylsulfonylphpymt)_2(\mu\text{-}Br)_2]_n$, respectively. Overlay drawings of the asymmetric units of **1Cu** with **3Cu** (Figure 1) and **3Cu** with **6Cu** (Figure 2) illustrate the similarities in the polymers.

The substitution of the phenyl ligand at its para position by a methoxy group (**3Cu**) and a methylsulfonyl group (**6Cu**) did not affect the formation of the polymer or its solid state structure. It is worth noting that the phenyl group of the phenylpyrimidine ligand is relatively free to rotate around the central carbon-carbon bond and can use different conformations to reduce the crystal packing forces or to allow intermolecular interactions. In the structure of **6Cu**, the rotation of the terminal ligands created voids in the crystal that were large enough to host solvent molecules of water.

Photooxidation studies

With the aim of achieving *in cellulo* photooxidation of essential molecules such as GSH, the photocatalytic ability of the copper(I) clusters has been evaluated on the oxidation of cysteine, an amino acid which oxidizes into a dimer with a disulfide bond, just like GSH. Photocatalytic conversion of boronic acids into phenols has been previously described with **1Cu**, and was ascribed to the formation of superoxide from oxygen.[20] The catalytic ability to oxidize thiols has thus been investigated with complexes **1Cu**–**6Cu** (4 mol%) upon light irradiation (450 nm, 25 $mW.cm^{-2}$) and in the dark in a 1:1 D_2O/CD_3CN mixture with 100 mM cysteine. The reaction was followed by ^{1}H-NMR spectroscopy[21] by analyzing the conversion with 1,4-dioxane as a reference (11 mM). All complexes showed good catalytic activity upon light irradiation while remaining completely inactive in the dark. The cysteine concentration over time is depicted in Figure 3. Cysteine is likely partly oxidized by peroxide species. Such a reaction would be limited by the concentration of dioxygen in the solvents, which might explain the slow reaction rate. We note that the reaction rates tend to follow the Hammett equation tendency: **6Cu** > **5Cu** > **1Cu** > **2Cu**. Moreover, the phenol of **2Cu** could be subject to competitive oxidation, which would explain, in this

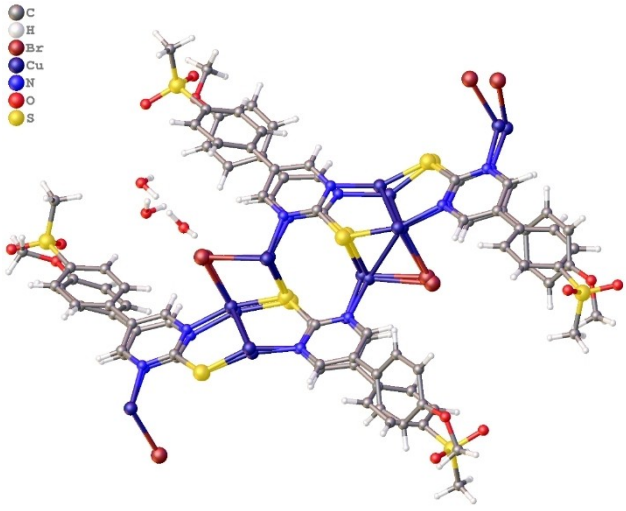

Figure 2. Overlay drawing of the molecular structures of **3Cu** and **6Cu**.

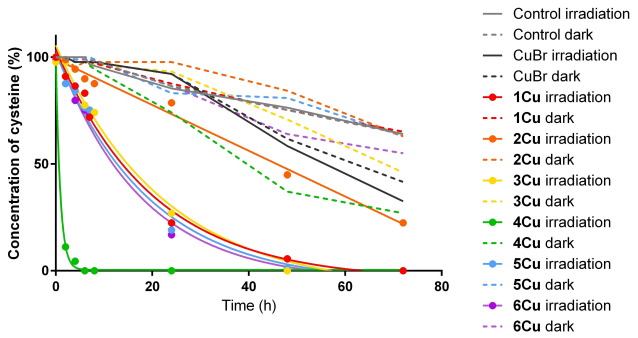

Figure 3. Cysteine concentration (determined by NMR conversion against a dioxane reference) as a function of time for the photocatalytic oxidation of cysteine upon 450 nm irradiation (25 mW.cm^{-2}). Exponential fit ($r^2 = 0.99$) for the data corresponding to irradiated reactions. Dashed lines are for dark controls.

case, the very slow oxidation of cysteine. Surprisingly, the chloro-appended **4Cu** is exceptionally active compared to others, inducing complete conversion of cysteine after 6 h of 450 nm irradiation. We note that this compound is much more soluble in common organic solvants (1 mg/mL in MeCN vs 0.2 mg/mL for other compounds). It is likely that **4Cu** crystallizes according to a different structure, perhaps with a smaller number of copper units and ligands, which would explain **4Cu**'s better solubility, and therefore better photocatalytic activity. The size of particules in the biological medium used for the cellular assays has been measured with Dynamic Light Scattering. All suspended particles are about 8 nm (see Supporting Information), except for **4Cu**, which forms much larger particles, confirming the hypothesis of a different structure for this compound.

Unfortunately, despite numerous attempts, elucidating the crystal structure of this compound remained elusive.

In order to set conditions closer to those in which the biological tests will be carried out, the photo-oxidation of GSH with the copper complex was studied for 8 minutes only (Table S1), as irradiation at 450 nm for a longer time tends to damage cells (< 95% survival after 8 minutes). The cells were therefore irradiated with a total dose of 1.86 J.cm^{-2} only. In those conditions, we nevertheless observed a conversion under light irradiation for **3Cu** (23%), **5Cu** (14%), **6Cu** (20%), and the highest conversion for the most active compound, **4Cu** (45%). We note that **1Cu** and **2Cu** did not induce any oxidation of GSH after 8 minutes of irridation. Assuming that such a disruption of the cell's redox equilibrium would be sufficient to induce cell death, we studied the photocytoxicity of the six copper compounds at 450 nm.

Photocytotoxicity studies

Encouraged by the results previously described, the photocytotoxicity of the compounds was investigated on murine colorectal cancer cells (CT26). After 4 h of incubation, with and without renewal of the medium, the cells were irradiated for 8 min at 450 nm (1.86 J.cm^{-2}) – with a control in the dark. The cytotoxicity was determined using the resazurin assay 48 h in total after incubation. However, none of the compounds showed any toxicity at concentrations up to 100 μM, with or without light irradiation, after 4, 24, and even 48 h incubation. This might be due to the very poor solubility of the oligomeric clusters in biological medium. Additionally, it is also possible that the 8 minutes of 450 nm irradiation were not sufficient for inducing a significant redox imbalance in the cell, despite the GSH to GSSG conversions observed. Indeed, it corresponds to an energy of only 1.86 J.cm^{-2} overall, which is much less than what can be achieved with higher wavelengths, as previously demonstrated in our group (6.7 J.cm^{-2} for 60 min of irradiation at 620 nm).[22]

Conclusions

In this study, the photoredox and biological evaluation of six copper(I) thiol clusters was reported. The clusters crystallized in an oligomeric structure, were highly stable towards air and moisture, and showed excellent photooxidation of cysteine and GSH upon 450 nm irradiation. Biological studies on CT26 cells showed no phototoxicity of the compounds, probably because of low cellular uptake and irradiation times. Yet, the excellent photoredox properties of the compounds are encouraging and prompted us to further investigate the activity of such compounds for biological applications. If similar compounds could achieve higher absorption wavelengths, it would be possible to irradiate for longer times, which would be more likely to induce a significant redox imbalance. In order to improve the cellular uptake, encapsulation, which can greatly enhance the biological profile of metal-based drugs,[23] would constitute a valuable strategy.

Experimental Section

General remarks. Chemicals were purchased from Sigma Aldrich, or TCI chemicals. ^{1}H and ^{13}C NMR spectra were recorded in deuterated solvents on Bruker 400 or 500 MHz spectrometer at room temperature. The chemical shifts, δ, are reported in ppm (parts per million). The residual solvent peaks have been used as internal references. The abbreviations for the peak multiplicities are as follows: s (singlet), d (doublet), t (triplet), m (multiplet). All IR spectra were recorded using a *Nicolet 380* model *FT-IR* spectrometer. UV-vis spectra were recorded using a Cary 3500 UV-vis spectrophotometer. Solvothermal reactions were carried out in a Nabertherm programmable oven (Muffle furnace L 1/12). Cyclic voltammogram (CV) experiments were carried out using. The electrochemical measurements were performed on **4Cu** (1.0 mM) in an acetonitrile solution containing tetrabutylammonium hexafluorophosphate (0.1 M) as supporting electrolyte. The solutions were degassed under argon and cyclic voltammograms were scanned from −1.6 V to +1.6 V with a PGSTAT100 potentiostat. The three-electrode system was used: a glassy carbon electrode as the working electrode, SCE as the reference electrode, and a Pt wire as the counter electrode. CV was performed at a scan rate of 100 mV/s. IR spectra were recorded on an Agilent Cary 600 Series FTIR Spectrometer with a PIKE GladiATR module. The photocalytic oxidation of cysteine and glutathione was carried out under 450 nm irradiation with a

Thorlabs N450LP1 lamp (25 mW.cm^{-2}). The elemental analysis have been performed with a CHNS ELEMENTAR Vario apparatus.

Single crystal X-ray diffraction data were collected at 160(1) K on Rigaku OD diffractometers (Synergy/Hypix for **1Cu** and **6Cu**; Supernova/Atlas for **3Cu**) using the copper X-ray radiation (I = 1.54184 Å) from a dual wavelength X-ray source and an Oxford Instruments Cryojet XL cooler. The selected suitable single crystal was mounted using polybutene oil on a flexible loop fixed on a goniometer head and immediately transferred to the diffractometer. Pre-experiments, data collections, data reductions, and analytical absorption corrections[24] were performed with the program suite *CrysAlisPro*.[25] Using *Olex2*,[26] the structure was solved with the SHELXT[27] small molecule structure solution program and refined with the *SHELXL2018/3* program package[28] by full-matrix least-squares minimization on F^2. *PLATON*[29] was used to check the results of the X-ray analyses. Deposition Numbers 2277452 (**1Cu**), 2277454 (**3Cu**), and 2277453 (**6Cu**) contain the supplementary crystallographic data for this paper. These data are provided free of charge by the joint Cambridge Crystallographic Data Centre and Fachinformationszentrum Karlsruhe Access Structures service.

Synthesis of vinamidinium precursors.[30] In a 50 mL flask, the arylacetic acid (6 mmol) was dissolved in 5 mL DMF and cooled at 0 °C (ice bath). $POCl_3$ (3 equiv.) was added dropwise and the mixture was stirred for 15 minutes. The mixture was then heated at 90 °C for 5 hours. The reaction mixture was then poured into 100 g of crushed ice and 3 equiv. of NH_4PF_6 (3.5 mL of a 5 M solution in water) were added dropwise. The off-white solid obtained was filtered and washed with water. Additional compound was extracted from the filtrate with dichloromethane. The organic layer was then concentrated under vacuum and the solid fractions were combined.

Ligand synthesis.[31] In a 50 mL flask, the vinamidinium precursor (3.3 mmol) and thiourea (5 mmol, 1.5 equiv.) were dissolved in 10 mL of absolute ethanol. Subsequently, MeONa (2 equiv, 6.6 mL of a 1 M solution in methanol) was added and the reaction mixture was stirred at r.t. for 0.5 h and then refluxed for 18 h. After cooling to r.t. acetic acid (2 mL, 33 mmol, 10 equiv.) was added. The bright yellow precipitate was separated, washed with water, and dried.[31]

Clusters synthesis. Amorphous powder. In a sealable tube, equipped with a magnetic stirrer, CuBr and the ligands (0.075 mmol) were added. MeCN (4.0 mL) was then added and the mixture was degassed by bubbling N_2. The tube was then sealed and heated in an oil bath at 120 °C for 48 h and then cooled to room temperature. The red solid was filtered and washed with MeCN. The compound obtained is insoluble in most common solvents. **Crystals**. In a sealable flask, the ligand phpymt (0.08 mmol) and copper bromide (15.7 mg, 0.08 mmol) were introduced. MeCN (2.0 mL) was then added and the mixture was degassed by bubbling N_2 (the mixture turns from orange to yellow). Then, 1 drop of triethylamine was added and the flask was sealed. The mixture was heated at 120 °C in a programmable oven for 48 h. The temperature was then decreased slowly (5 °C per hour) until it reached room temperature. The dark orange crystals obtained were filtered and dried.

Photocatalytic oxidation of cysteine. In a test tube, 100 μmol of cysteine with 11 μmol dioxane (1 mg) in 1 mL D_2O and 4 μmol of copper catalyst (molecular weight calculated using the single unit formula L_2CuBr) in 1 mL CD_3CN were introduced. The reaction was stirred upon 450 nm irradiation (25 mW.cm^{-2}) at 25 °C with an additional tube in the dark for control. For the NMR follow-up, 100 μL were taken and quenched with 500 μL D_2O. Cysteine signal: ^{1}H NMR (500 MHz, D_2O) δ 3.94 (dd, J = 5.8, 4.1 Hz, 1H), 3.07 (dd, J = 14.9, 5.8 Hz, 1H), 2.99 (dd, J = 14.9, 4.1 Hz, 1H). Cystine signal: ^{1}H NMR (500 MHz, D_2O) δ 4.09 (dd, J = 8.3, 3.8 Hz, 1H), 3.36 (dd, J = 15.1, 3.8 Hz, 1H), 3.16 (dd, J = 15.1, 8.3 Hz, 1H). Dioxane (reference): ^{1}H NMR (500 MHz, D_2O) δ 3.73 (s, 1H).

Supporting Information

The authors have cited additional references within the Supporting Information.[30,31]

Acknowledgements

L.G.G. thanks the ENS-PSL for her PhD fellowship. This work was also financially supported by an ERC Consolidator Grant Photo-MedMet to G.G. (GA 681679), who has received support under the program "Investissements d'Avenir" launched by the French Government and implemented by the ANR with the reference ANR-10-IDEX-0001-02 PSL (G.G.). The authors thank Dr. Domitille Giaume (Chimie ParisTech, PSL University) for lending the programmable oven, which yielded crystals suitable for X-ray diffraction. The authors also thank the following researchers for giving us access to their apparatus: Dr. Laurence Grimaud (ENS, PSL University) for the cyclic voltammetry, Dr. Blaise Dumas (ENS, PSL University) for the fluorometer, and Dr. Gregory Lefevre (Chimie ParisTech, PSL University) for the Dynamic Light Scattering.

Conflict of Interests

The authors declare no conflict of interest.

Data Availability Statement

The data that support the findings of this study are available from the corresponding author upon reasonable request.

Keywords: Cu(I) clusters · cysteine · GSH balance · photo-oxidation

[1] E. Boros, P. J. Dyson, G. Gasser, *Chem* **2020**, *6*, 41–60.
[2] B. Rosenberg, L. Vancamp, J. E. Trosko, V. H. Mansour, *Nature* **1969**, *222*, 385–386.
[3] Y. Fang, Z. Zhang, *Cell. Mol. Biol. Lett.* **2020**, *25*, 44.
[4] F. H. Abdalbari, C. M. Telleria, *Discov. Oncol.* **2021**, *12*, 42.
[5] D. Dolmans, D. Fukumura, R. K. Jain, *Nat. Rev. Cancer* **2003**, *3*, 380–387.
[6] H. Huang, S. Banerjee, K. Qiu, P. Zhang, O. Blacque, T. Malcomson, M. J. Paterson, G. J. Clarkson, M. Staniforth, V. G. Stavros, G. Gasser, H. Chao, P. J. Sadler, *Nat. Chem.* **2019**, *11*, 1041–1048.
[7] L. Gourdon, K. Cariou, G. Gasser, *Chem. Soc. Rev.* **2022**, *51*, 1167–1195.
[8] C. Förster, K. Heinze, *Chem. Soc. Rev.* **2020**, *49*, 1057–1070.
[9] M. Rice, *Archaeol. Arab. Gulf* **1994**, 276–280.
[10] H. D. Nguyen, L. H. Do, *Curr. Opin. Chem. Biol.* **2022**, *71*, 102213.
[11] J. L. Stauber, T. M. Florence, *Mar. Biol.* **1987**, *94*, 511–519.
[12] A. Santoro, J. S. Calvo, M. D. Peris-Díaz, A. Krężel, G. Meloni, P. Faller, *Angew. Chem.* **2020**, *132*, 7904–7909.
[13] A. Hossain, A. Bhattacharyya, O. Reiser, *Science* **2019**, *364*, DOI:10.1126/science.aav9713.

[14] K. Ngamchuea, C. Batchelor-McAuley, R. G. Compton, *Chem. Eur. J.* **2016**, *22*, 15937–15944.
[15] A. Rigo, A. Corazza, M. Luisa di Paolo, M. Rossetto, R. Ugolini, M. Scarpa, *J. Inorg. Biochem.* **2004**, *98*, 1495–1501.
[16] A. Santoro, N. E. Wezynfeld, M. Vašák, W. Bal, P. Faller, *Chem. Commun.* **2017**, *53*, 11634–11637.
[17] E. Falcone, F. Stellato, B. Vileno, M. Bouraguba, V. Lebrun, M. Ilbert, S. Morante, P. Faller, *Metallomics* **2023**, mfad040.
[18] S.-D. Hong, T.-Q. Yu, B. Guo, H.-Y. Li, H.-X. Li, *J. Mol. Struct.* **2021**, *1227*, 129420.
[19] X.-Q. Liang, R. K. Gupta, Y.-W. Li, H.-Y. Ma, L.-N. Gao, C.-H. Tung, D. Sun, *Inorg. Chem.* **2020**, *59*, 2680–2688.
[20] M.-J. Zhang, H.-X. Li, H.-Y. Li, J.-P. Lang, *Dalton Trans.* **2016**, *45*, 17759–17769.
[21] F. Giannini, G. Süss-Fink, J. Furrer, *Inorg. Chem.* **2011**, *50*, 10552–10554.
[22] A. Mani, T. Feng, A. Gandioso, R. Vinck, A. Notaro, L. Gourdon, P. Burckel, B. Saubaméa, O. Blacque, K. Cariou, J.-E. Belgaied, H. Chao, G. Gasser, *Angew. Chem. Int. Ed.* **2023**, *62*, e202218347.
[23] E. Villemin, Y. C. Ong, C. M. Thomas, G. Gasser, *Nat. Chem. Rev.* **2019**, *3*, 261–282.
[24] R. C. Clark, J. S. Reid, *Acta Crystallogr. Sect. A* **1995**, *51*, 887–897.
[25] *CrysAlisPro* software (version 1.171.42.75a), Rigaku Oxford Diffraction Ltd, Yarnton, Oxfordshire, England, 2022.
[26] O. V. Dolomanov, L. J. Bourhis, R. J. Gildea, J. A. K. Howard, H. Puschmann, *J. Appl. Crystallogr.* **2009**, *42*, 339–341.
[27] G. M. Sheldrick, *Acta Crystallogr. Sect. Found. Adv.* **2015**, *71*, 3–8.
[28] G. M. Sheldrick, *Acta Crystallogr. Sect. C Struct. Chem.* **2015**, *71*, 3–8.
[29] A. L. Spek, *Acta Crystallogr. D Biol. Crystallogr.* **2009**, *65*, 148–155.
[30] S. Selvi, P. T. Perumal, *Tetrahedron Lett.* **1997**, *38*, 6263–6266.
[31] J. G. Sośnicki, Ł. Struk, M. Kurzawski, M. Perużyńska, G. Maciejewska, M. Droździk, *Org. Biomol. Chem.* **2014**, *12*, 3427–3440.

Manuscript received: July 5, 2023
Revised manuscript received: September 13, 2023
Accepted manuscript online: September 26, 2023
Version of record online: October 16, 2023